Antibody-functionalised gold nanoparticles-based impedimetric immunosensor: detection methods for better sensitivity

Nadra Bohli[1] ✉, *Meryem Belkilani*[1,2], *Laurence Mora*[3], *Adnane Abdelghani*[1]

[1]*Carthage University, National Institute of Applied Science and Technology, Research Unit of Nanobiotechnology and Valorisation of Medicinal Plants UR17ES22, Bp 676, Centre Urbain Nord, 1080 Charguia Cedex, Tunisia*
[2]*Tunis University, ENSIT, Avenu Taha Hussein, Montfleury, 1008 Tunis, Tunisia*
[3]*Université Paris13, Institut Galilée, Sorbonne Paris Cité, F-93430 Villetaneuse, France*
✉ *E-mail: nadra.bohli@insat.u-carthage.tn*

Published in Micro & Nano Letters; Received on 25th September 2018; Revised on 20th January 2019; Accepted on 11th February 2019

Electrochemical immunosensors are generally layer-by-layer or sandwich systems designed to detect an analyte in a solution. Immunosensors are mainly based on the high affinity and specificity of the antibody towards its antigen. This work aims to answer the following question: if we 'flip' the immunosensor and build it backwards, thus detecting the antibody with the antigen instead of detecting the antigen with the antibody, will we obtain the same immunosensors properties or not? To answer this question, they tested a system composed of glycated human serum albumin and antibody-functionalised gold nanoparticles. Impedance spectrum results showed a difference in both the sensitivity and linear range of the built impedimetric immunosensors. The sensitivity of the sensor using the antibody as a bioreceptor was approximated to 0.32 [%. [% (Glycated to total albumin])] − 1] against a sensitivity of 0.80 [%. [% (Glycated to total albumin])] − 1] for the 'upside-down' sensor, using the antigen as a bioreceptor. This study observed also a shift to high glycation levels in the linear range of the upside-down sensor. These differences could be explained by the effect of steric hindrance and a higher degree of freedom allowing better characteristics for the upside-down immunosensor.

1. Introduction: Electrochemical biosensors have attracted a lot of interest in the scientific community as they lead to the development of simple, rapid, reliable and inexpensive point of care testing devices enabling early clinical diagnosis [1]. An electrochemical biosensor consists of a biochemical receptor in contact with an electrochemical transducer [2]. The bioreceptor can be a microbe-based containing micro-organisms, an enzyme, a nucleic acid or an antibody [3, 4].

Antibody-based electrochemical biosensors, usually referred to as immunosensors, have been widely explored in the literature mainly owing to the very high equilibrium association constants achievable between an antibody and its corresponding antigen. An antibody is a 'Y' shaped molecule, where the arms are identical polypeptide chains responsible for antigen binding (antigen binding fragments or domains Fab), and the tail is the crystallisable fragment (Fc fragment or domain). Several parameters come into consideration in the design of an immunosensing device and can affect important features like its sensitivity, detection limits or linear range of detection. Antibody immobilisation strategies, for instance, can influence the orientation and accessibility of antibody binding sites and/or the strength of the electrostatic interactions between antibodies and sensing platform leading to a difference in the immunosensor performance.

The detailed considerations promoting the immobilisation and the right orientation can be found in several recent studies [5–11] and therefore will only be concisely discussed. The immobilisation of the antibody is generally done directly on the sensing surface either by physical adsorption or by chemical bonds. Magnetic or metallic nanoparticles can be used to enhance the immunosensor sensitivity by increasing the rate of electron transfer at the bio-interface [12–16].

The immunosensor building is generally performed by multistep protocol based on a layer-by-layer films approach and consists of immobilising the antibody and detecting its associated antigen [17]. The use of the antibody as a bioreceptor is very common in publications either for medical diagnosis or environmental monitoring [18, 19]. However, little work was found using the antigen as a bioreceptor and it was mainly specific to antibody detection [20]. Andersen *et al*., for instance, designed a single-step gold nanoparticle (AuNP) based immunoassay in which they tagged the nanoparticles surface with a short viral peptide epitopes and detected the associated antibody through a colorimetric response triggered by the aggregation of the immune complex [21].

To the best of our knowledge, for electrochemical biosensors no study was undertaken to explore whether there would be a change of performance if we inverse the system by immobilising the antigen and detecting its corresponding antibody.

Hence, in this Letter, we propose to compare and study these two strategies. The system chosen is an immunosensor for glycated albumin (GA). Here we propose for the antibodies to be immobilised in AuNPs through physical adsorption. AuNPs were chosen for their biocompatibility in contrast with other NPs such as metal oxides and carbon nanotubes, found to be toxic for cells in many vitro studies. Physical adsorption was used as this immobilisation technique generally avoids the use of reagents and decreases the chances of protein denaturation [14].

2. Materials and methods: AuNPs were supplied by Pr. Sherine Obare Group (Michigan University, USA) [22, 23]. The AuNPs were synthesised by the reduction of $HAuCl_4$ using sodium borohydride ($NaBH_4$). More details can be found in [22–24]. The anti-human serum albumin monoclonal antibody (Ab) was purchased from ABBIOTEC (USA). The antigen tested is human serum albumin prepared at six different glycation levels, which are 0, 7.49, 15.79, 22.56, 46.50 and 66.73% (GA/total albumin). GA samples detailed preparation procedure is described in previous work [25].

CHI 604E impedance analyser (CH Instruments, USA) was used for cyclic voltammetry (CV) and electrochemical impedance spectroscopy (EIS) measurements with three separate electrodes electrochemical cell. The working, counter and reference electrodes were, respectively, gold microelectrode, platinum and saturated Ag/Ag-Cl electrodes. The frequency covered 100 mHz to 100 kHz interval, at 0.1 V DC potential versus the reference electrode with a 10 mV modulation voltage.

The gold electrodes, procured in France from Laboratoire d'Analyse et d'Architechture des Systèmes, were dipped in acetone for 10 min in an ultrasonic bath, rinsed with ultrapure water, then immersed in a piranha solution (3:1 (v/v) 95% H_2SO_4/H_2O_2) for 20 min. Finally, they were thoroughly rinsed with ultra-pure water and dried under a nitrogen flow. After cleaning, each gold electrode was immediately placed as working electrode on the three separate electrodes electrochemical cell. All measurements were performed at room temperature, in a phosphate buffered saline solution with $K_4Fe(CN)_6^{3-}/K_4Fe(CN)_6^{4-}$ redox couple at 5 mM concentration. Further details on materials and methods are to be found in [26, 27].

3. Results and discussion

3.1. Detecting antigen with antibody

3.1.1. Sensor building: The immunosensor is a multilayer structure containing antibody-functionalised AuNPs (AuNPs-Ab) physisorbed on the gold electrode, on which we added bovine serum albumin (BSA) layer and finally the antigen layers (added from the lowest to the highest glycation level). The schematic representation of the fabrication process of the multilayer system of the immunosensor on the gold electrode is presented in Fig. 1.

3.1.2. Characterisation of the immunosensor layers: EIS and CV were performed to characterise all added layer. In CV, we scan the working electrode potential with a triangular potential waveform and measure the resulting current. Cyclic voltammograms of bare gold microelectrode, AuNPs functionalised with monoclonal antibody to human serum albumin and gold/AuNPs-Ab/BSA layers are shown in Fig. 2.

Through Fig. 2, we observe the reversible nature of cyclic voltammogram of the bare gold electrode, with the oxidoreduction characteristic current peaks. The peaks intensities faded away while adding AuNPs-Ab layer and then BSA layer.

EIS measurements, generally used for the analysis of the electrode/electrolyte interfacial reaction mechanisms, confirmed the successful immobilisation of each layer on the working electrode as shown in Fig. 3.

As displayed by the Nyquist plots in Fig. 3, the charge transfer resistance (R_{ct}) at the electrode/electrolyte interface increased while adding AuNPs-Ab, and then BSA layers confirming then the CV results.

3.1.3. GA detection: Impedance measurements of different GA levels (10 ng/ml solution concentration) are shown in Fig. 4.

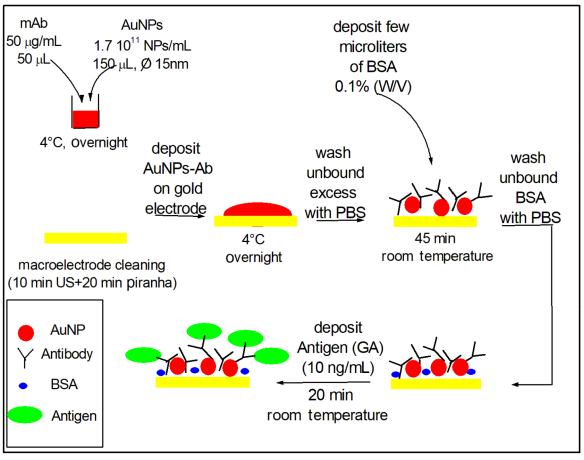

Fig. 1 *Schematic representation of the fabrication process of the multilayer system of the immunosensor on the gold electrode*

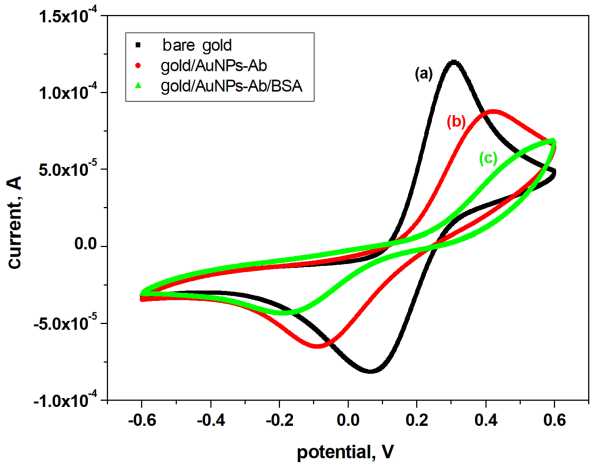

Fig. 2 *CV of immunosensor layers*
a Bare gold microelectrode
b Gold/AuNPs-Ab (AuNPs functionalised with Ab)
c Gold/AuNPs-Ab/BSA

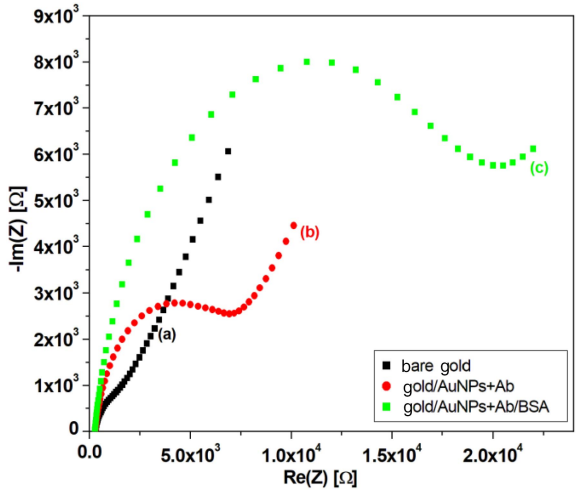

Fig. 3 *Impedance measurements of*
a Bare gold microelectrode
b Gold/AuNPs-Ab (antibody-functionalised AuNPs)
c Gold/AuNPs-Ab/BSA

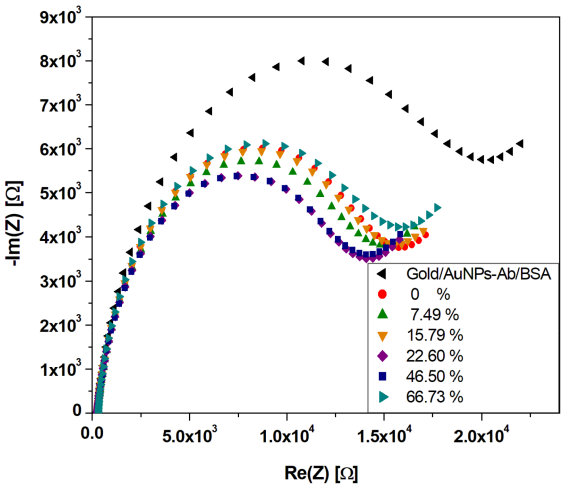

Fig. 4 *Impedance measurements of different GA levels at 10 ng/ml*

doi: 10.1049/mnl.2018.5587

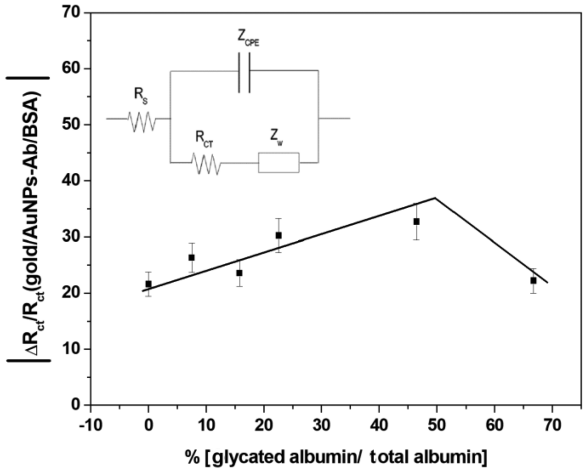

Fig. 5 *Immunosensor's calibration curve at 10 ng/ml concentration of different GA levels. The inset is the Randles equivalent electrical circuit*

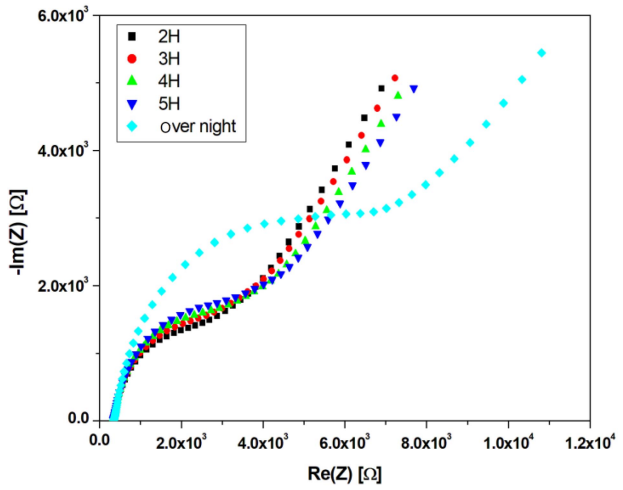

Fig. 6 *Impedance measurements of different deposition times of the antigen (GA level = 7.49%, 10 ng/ml)*

We observe from the Nyquist plots a decrease in R_{ct} upon the increase of albumin glycation level due to morphological changes [28].

The Nyquist curves were fitted to Randles circuit (inset Fig. 5). This electrical circuit is composed of the solution and connections resistance R_s, the charge transfer resistance R_{ct}, the Warburg impedance Z_w and the constant phase element Z_{CPE}.

Calibration curve data were calculated according to the following equation:

$$\left|\frac{\Delta R_{ct}}{R_{ct}(\text{gold/AuNps} - \text{Ab/BSA})}\right| = \left|\frac{R_{ct}(\text{GA}) - R_{ct}(\text{gold/AuNps} - \text{Ab/BSA})}{R_{ct}(\text{gold/AuNps} - \text{Ab/BSA})}\right| \quad (1)$$

The calibration curve, consisting of the variation of

$$\left|\frac{\Delta R_{ct}}{R_{ct}(\text{gold/AuNps} - \text{Ab/BSA})}\right|$$

versus GA levels, is presented in Fig. 5.

In Fig. 5, the sensor sensitivity value was approximated to 0.32 [%. [% (Glycated to total albumin])]$^{-1}$].

As the immunosensing principle is based on the specific molecular recognition between the antibody and the antigen, we propose in the second part of this Letter to study the properties of the sensor if the recognition is done on the other direction that is to say detecting the antibody by the antigen.

3.2. Detecting the antibody with antigen: upside-down immunosensor

3.2.1. Sensor building: The proposed immunosensor is a multilayer structure containing the same layers presented in the first part of the Letter but arranged in a different manner. In this part of the study, we began by adding the antigen on the gold surface (by physisorption, 10 ng/ml concentrated sample) and left it to incubate overnight at room temperature (20°C). The incubation time used for the antigen was found through an optimisation step in which we measured the impedance of that added antigen layer at different times of incubation ranging from 2 h to an overnight period of time (an average of 18 h). The Nyquist plots related to this optimisation procedure are displayed in Fig. 6.

Then we added BSA layer by incubating 100 µl of BSA solution (0.1%, w/v) onto the sensors for 45 min. Finally, we added a mixture AuNPs-Ab-BSA containing AuNPs-Ab and BSA. To achieve this mixed structure, we first began by preparing the AuNPs-Ab by adding 50 µl of Ab (50 µg/ml) to 150 µl of AuNPs dispersion (concentration of 1.7 1011 NPs/ml, average diameter of 15 nm).

The solution components were left to react at 4°C overnight. Then we prepared 100 µl of AuNPs-Ab-BSA by adding two equal volumes of AuNPs-Ab solution and BSA solution (0.1%, v/w) and left them to react for at least 45 min. The addition of BSA to the functionalised antibody AuNPs was meant to block any uncovered AuNP surface and thus to prevent eventual unspecific binding. A drop of the AuNPs-Ab-BSA solution was put onto the gold microelectrode and left to incubate for 20 min.

The schematic representation of the fabrication process of the multilayer system of the immunosensor on the gold electrode is presented in Fig. 7.

3.2.2. Detection of the antibody: The cyclic voltammograms and Nyquist plots measured after each layer deposition are displayed respectfully in Figs. 8 and 9.

A distinct change is observed either in the CV plots or in the Nyquist plots after the immobilisation of each layer. These changes refer to a decrease of the oxydoreduction peaks and to an increase in the diameter of the Nyquist distinctive semi-circle, implying an increase of R_{ct} upon layers addition. This behaviour was observed for several antigens tested.

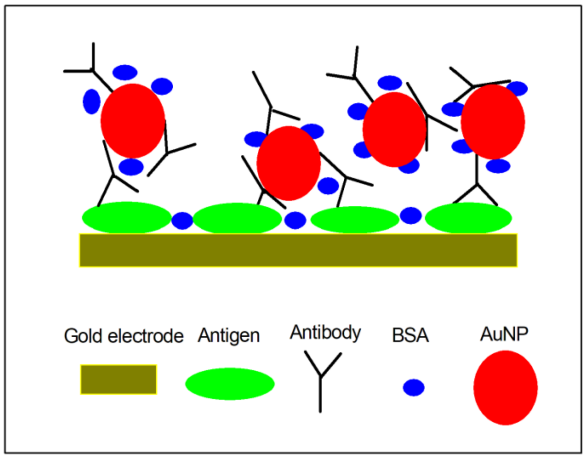

Fig. 7 *Schematic representation of the multilayer system of the 'upside-down' immunosensor on the gold electrode*

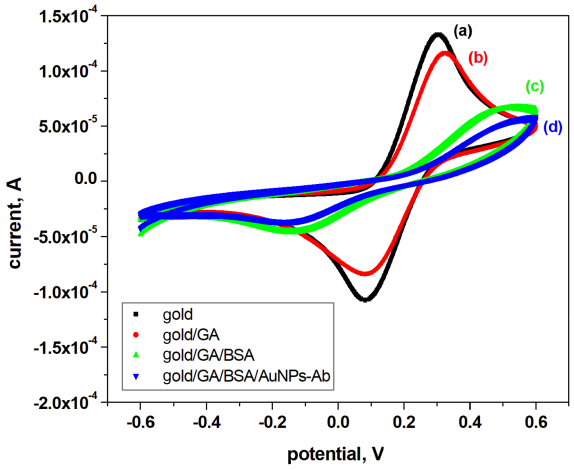

Fig. 8 *CV of the 'upside-down' immunosensor's layers*
a Bare gold microelectrode
b Gold/GA
c Gold/GA/BSA
d Gold/GA/BSA/AuNPs-Ab-BSA

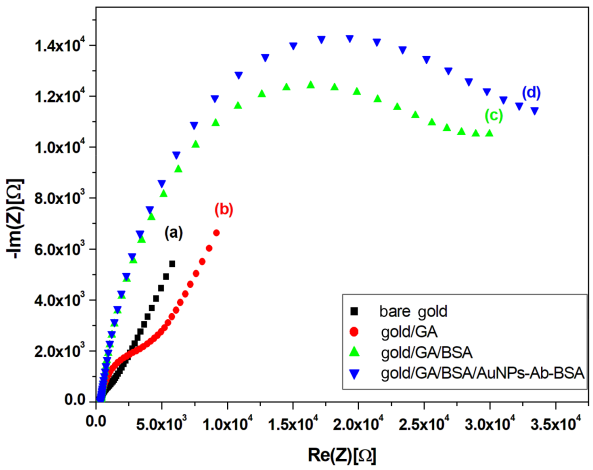

Fig. 9 *Impedance measurements of the different 'upside-down' immunosensor's layers*
a Bare gold electrode
b Gold/antigen
c Gold/GA/BSA
d Gold/GA/BSA/AuNPs-Ab-BSA

Calibration curve data were calculated according to the following equation:

$$\left|\frac{\Delta R_{ct}}{R_{ct}(\text{gold/GA/BSA})}\right| = \frac{R_{ct}(\text{AuNPs} - \text{Ab} - \text{BSA}) - R_{ct}(\text{gold/GA/BSA})}{R_{ct}(\text{gold/GA/BSA})} \quad (2)$$

The corresponding calibration curve is presented in Fig. 10 and displays

$$\left|\frac{\Delta R_{ct}}{R_{ct}(\text{gold/GA/BSA})}\right|$$

versus GA level. For a clearer comparison, the former calibration curve is superimposed on Fig. 10. According to Fig. 10, the 'upside-down' sensor sensitivity value was approximated to 0.8 [%. [% (Glycated to total albumin])]$^{-1}$]. This observation is quite different from that found in the first part of the study. The sensor is yet more sensitive but not for the same glycation ratio interval.

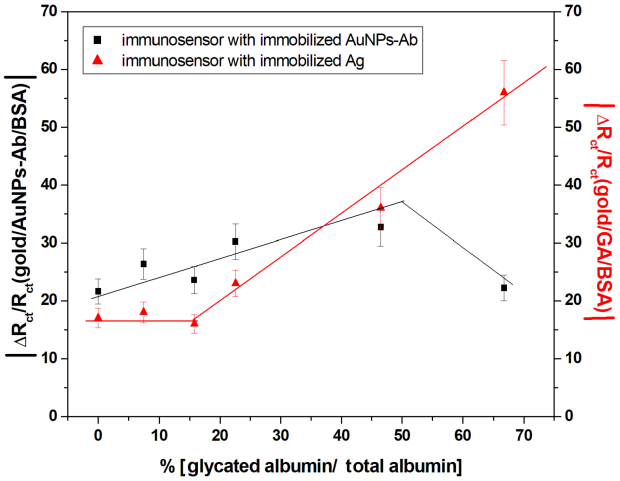

Fig. 10 *Calibration curves of both immunosensors at 10 ng/ml concentration at several GA levels*

There are a number of possible explanations for these observations. One possible reason is related to the antibody binding efficiency through its adsorption onto the AuNPs. This binding efficiency is strongly related to the availability of the Fab domain to interact with the antigen. Generally, the protein adsorption onto the AuNPs surface is mostly regulated by van der Waals force, hydrophobic interaction, electrostatic interaction and hydrogen bonding, and also by the structural rearrangements (driven by the reduction of the overall free energy of the system) [29]. It is also dependent on the nanoparticle size. For low diameter AuNPs (10–15 nm), previous studies [30] on IgG antibodies demonstrated that they attach to AuNPs through Fc domain, leaving the Fab part pointed into the solution. So, it is more likely that the antigen binding domains are quite available in our case. Moreover, for the upside-down immunosensor, the AuNPs allow a certain degree of freedom for the attached antibodies so that they can find more easily a matching antigen on the gold electrode. For the classical immunosensor, however, as the AuNPs-Ab are physisorbed onto the gold electrode surface, different configurations are possible and a steric hindrance of the active part of the antibody is more likely to happen.

4. Conclusion: For an immunosensor, ideally, the antibody must be immobilised with the antigen binding sites sterically available and in its native form to allow a maximum number of binding antigens. To accomplish this purpose, numerous studies were conducted to identify key processing conditions responsible for the final overall features of the immunosensor.

Optimised buffer conditions, appropriate antibody immobilisation through the right choice of functional groups and ligands to the substrate surface are among the conditions that were studied in the literature. In this Letter, we found that the sensors layer-by-layer building protocol influences its final properties.

This result was achieved through a comparison between two immunosensor dispositions: the classic one using the antibody as a bioreceptor or an 'upside-down' disposition where the antigen is used as a bioreceptor. AuNPs were used to extend the sensitivity of the device. The calibration curves obtained from impedance measurements showed a sensor sensitivity value approximated to 0.32 [%. [% (Glycated to total albumin])]$^{-1}$] for the first disposition against a sensitivity of 0.80 [%. [% (Glycated to total albumin])]$^{-1}$] for the 'upside-down' sensor. The sensors linear ranges showed also a difference, where it seems that the upside-down sensor is more sensitive to high glycation levels (above 22.56% of glycated to total albumin).

doi: 10.1049/mnl.2018.5587

These observations confirm that when it comes to biosensors and macromolecules detection, we have to keep in mind that every step of the processing is important and can lead to changes as the biomolecule's conformations are dynamic overtime and can be influenced by the history of the sensors building protocol.

5. Acknowledgments: The authors gratefully acknowledge professors Olivier Meilhac, Philippe Rondeau who provided them the glycated albumin samples and Pr. Sherine Obare for collaboration under NSF project (grant no. 0909085).

6 References

[1] Bahadır E.B., Sezgintürk M.K.: 'Applications of electrochemical immunosensors for early clinical diagnostics', *Talanta*, 2015, **132**, pp. 162–174
[2] Thevenot D. R., Toth K., Durst R. A., *ET AL.*: 'Electrochemical biosensors: recommended definitions and classification', *Anal. Lett.*, 2001, **34**, pp. 635–659
[3] Perumal V., Hashim U.: 'Advances in biosensors: principle, architecture and applications', *J. Appl. Biomed.*, 2014, **121**, p. 15
[4] Santos A., Davis J. J., Bueno P. R.: 'Fundamentals and applications of impedimetric and redox capacitive biosensors', *J. Anal. Bioanal. Tech.*, 2014, **S7**, p. 16
[5] Ricci F., Adornetto G., Palleschi G.: 'A review of experimental aspects of electrochemical immunosensors', *Electrochim. Acta*, 2012, **84**, pp. 74–83
[6] Makaraviciute A., Ramanaviciene A.: 'Site-directed antibody immobilization techniques for immunosensors', *Biosens. Bioelectron.*, 2013, **50**, pp. 460–471
[7] Gopinath S. C. B., Tang T.-H., Citartan M., *ET AL.*: 'Current aspects in immunosensors', *Biosens. Bioelectron.*, 2014, **57**, pp. 292–302
[8] Trilling A. K., Beekwilder J., Zuilhof H.: 'Antibody orientation on biosensor surfaces: a minireview', *Analyst*, 2013, **138**, pp. 1619–1627
[9] Welch N. G., Scoble J. A., Muir B. W., *ET AL.*: 'Orientation and characterization of immobilized antibodies for improved immunoassays: review', *Biointerphases*, 2017, **12**, p. 02D301
[10] Luppa P. B., Sokoll L. J., Chan D. W.: 'Immunosensors–principles and applications to clinical chemistry', *Clin. Chim. Acta.*, 2001, **314**, pp. 1–26
[11] Wen W., Yan X., Zhu C., *ET AL.*: 'Recent advances in electrochemical immunosensors', *Anal. Chem.*, 2017, **89**, pp. 138–156
[12] Khashayar P., Amoabediny G., Larijani B., *ET AL.*: 'Fabrication and verification of conjugated AuNP-antibody nanoprobe for sensitivity improvement in electrochemical biosensors', *Sci. Rep.*, 2017, **7**, p. 16070
[13] Heddle J. G.: 'Gold nanoparticle-biological molecule interactions and catalysis', *Catalysts*, 2013, **3**, pp. 683–708
[14] Farka Z., Jurík T., Kovář D., *ET AL.*: 'Nanoparticle-based immunochemical biosensors and assays: recent advances and challenges', *Chem. Rev.*, 2017, **117**, pp. 9973–10042
[15] Lim S. A., Ahmed M. U.: 'Electrochemical immunosensors and their recent nanomaterial-based signal amplification strategies: a review', *RSC Adv.*, 2016, **6**, (30), pp. 24995–25014
[16] Cho I-H., Lee J., Kim J., *ET AL.*: 'Review current technologies of electrochemical immunosensors: perspective on signal amplification', *Sensors*, 2018, **18**, p. 207
[17] Iost R. M., Crespilho F. N.: 'Layer-by-layer self-assembly and electrochemistry: applications in biosensing and bioelectronics', *Biosens. Bioelectron.*, 2012, **31**, pp. 1–10
[18] Wang Y., Zhang Y., Wu D., *ET AL.*: 'Ultrasensitive label-free electrochemical immunosensor based on multifunctionalized graphene nanocomposites for the detection of alpha fetoprotein', *Sci. Rep.*, 2017, **7**, p. 42361
[19] Chammem H., Hafaid I., Bohli N., *ET AL.*: 'A disposable electrochemical sensor based on protein G for high-density lipoprotein (HDL) detection', *Talanta*, 2015, **144**, pp. 466–473
[20] Radecka H., Radecki J.: 'Label-free electrochemical immunosensors for viruses and antibodies detection-review', *J. Mex. Chem. Soc.*, 2015, **59**, (4), pp. 269–275
[21] Andresen H., Mager M., Grießner M., *ET AL.*: 'Single-step homogeneous immunoassays utilizing epitope-tagged gold nanoparticles: On the mechanism, feasibility, and limitations', *Chem. Mater.*, 2014, **26**, pp. 4696–4704
[22] Jana N. R., Gearheart L., Murphy C. J.: 'Seeding growth for size control of 5-40 nm diameter gold nanoparticles', *Langmuir*, 2001, **17**, pp. 6782–6786
[23] Jana N. R., Gearheart L., Obare S. O. J., *ET AL.*: 'Anisotropic chemical reactivity of gold spheroids and nanorods', *Langmuir*, 2002, **18**, pp. 922–927
[24] Baccar H., Mejri M.B., Hafaiedh I., *ET AL.*: 'Surface plasmon resonance immunosensor for bacteria detection', *Talanta*, 2010, **82**, pp. 810–814
[25] Baraka-Vidot J., Planesse C., Meilhac O., *ET AL.*: 'Glycation alters ligand binding, enzymatic, and pharmacological properties of human albumin', *Biochemistry*, 2015, **54**, pp. 3051–3062
[26] Bohli N., Meilhac O., Rondeau P., *ET AL.*: 'A facile route to glycated albumin detection', *Talanta*, 2018, **184**, pp. 507–512
[27] Barsoukov E., Macdonald J. R.: 'Impedance spectroscopy: theory, experiment, and applications' (Wiley, New York, 2005, 2nd edn.)
[28] Bohli N., Chammem H., Meilhac O., *ET AL.*: 'Electrochemical impedance spectroscopy on interdigitated gold microelectrodes for glycosylated human serum albumin characterization', *IEEE Trans. NanoBiosci.*, 2017, **16**, pp. 676–681
[29] Bhakta S. A., Evans E., Benavidez T. E., *ET AL.*: 'Protein adsorption onto nanomaterials for the development of biosensors and analytical devices: A review', *Anal. Chim. Acta.*, 2015, **872**, pp. 7–25
[30] Kaur K., Forrest J. A.: 'Influence of particle size on the binding activity of proteins adsorbed onto gold nanoparticles', *Langmuir*, 2012, **28**, pp. 2736–2744